Isotopes from fossil coronulid barnacle shells record evidence of migration in multiple Pleistocene whale populations

Larry D. Taylor[a,1], Aaron O'Dea[b], Timothy J. Bralower[c], and Seth Finnegan[a]

[a]Department of Integrative Biology, University of California, Berkeley, CA 94720; [b]Smithsonian Tropical Research Institute, Balboa, Republic of Panama; and [c]Department of Geosciences, Pennsylvania State University, University Park, PA 16802

Edited by Thure E. Cerling, University of Utah, Salt Lake City, UT, and approved February 15, 2019 (received for review May 22, 2018)

Migration is an integral feature of modern mysticete whale ecology, and the demands of migration may have played a key role in shaping mysticete evolutionary history. Constraining when migration became established and assessing how it has changed through time may yield valuable insight into the evolution of mysticete whales and the oceans in which they lived. However, there are currently few data which directly assess prehistoric mysticete migrations. Here we show that calcite $\delta^{18}O$ profiles of two species of modern whale barnacles (coronulids) accurately reflect the known migration routes of their host whales. We then analyze well-preserved fossil coronulids from three different locations along the eastern Pacific coast, finding that $\delta^{18}O$ profiles from these fossils exhibit trends and ranges similar to modern specimens. Our results demonstrate that migration is an ancient behavior within the humpback and gray whale lineages and that multiple Pleistocene populations were undertaking migrations of an extent similar to those of the present day.

cetacean | barnacle | migration | evolution | fossil

Most modern mysticete whales undertake annual migrations that allow them to feed in cool, seasonally productive, high-latitude waters in summer before returning to warm, tropical waters where they breed in winter. In the northeast Pacific, migration routes span from breeding areas in Central America, Mexico, and Hawaii to feeding areas in the Gulf of Alaska, Bering Sea, and California Current system (1, 2). These migrations link mysticete ecology to the processes which shape ocean productivity patterns, and short-term disruptions to these patterns induce corresponding changes in mysticete migratory behavior and distribution (3). During the Pliocene and Pleistocene the world's oceans became characterized by increasingly strong seasonal upwelling and patchy productivity distributions, and long-distance migrations are thought to have first become selectively favored at this time (4–8). The Plio-Pleistocene was also a pivotal time in mysticete evolution: Taxonomic diversity and morphological disparity decreased, most small-bodied forms disappeared, and gigantism became established across the clade (6, 7). Whether these evolutionary trends were driven by changing patterns of ocean productivity and selection for migratory adaptations remains an open question. Understanding when migration first became established, which ancient populations were migrating, and how stable the behavior has been through time may resolve questions of the significance of migration to mysticete evolution. However, we currently have little direct data regarding the migratory behaviors of prehistoric whale populations. Stable isotope systems can be useful in reconstructing animal movements (9), but these methods require a continuously growing tissue that has a high preservation potential and is resistant to diagenetic alteration. Tooth enamel has been used to reconstruct the movements of extinct odontocetes (10), but edentulous mysticetes have no comparable tissue. Several mysticete lineages play host to commensal barnacles, however, and $\delta^{18}O$ profiles collected from fossil whale barnacles may offer insight into ancient mysticete behaviors (11).

Coronulid barnacles belong to the superfamily Coronuloidea, which includes species adapted to live on turtles, manatees, crabs, and snakes (12). These barnacles live enclosed within a shell of six calcite plates and grow by depositing new material at the shell base, with the $\delta^{18}O$ values of each new growth increment determined primarily by the temperature and isotopic composition of the surrounding seawater (refs. 13 and 14 and *SI Appendix*, Fig. S1). A continuously growing barnacle can thus preserve an oxygen isotope signature of its host whale's movements, with a year's worth of shell growth recording an entire annual migration. This approach has been used to reconstruct the migration of modern-day turtles and California gray whales (14, 15). While several fossil specimens of the gray whale barnacle (*Cryptolepas rhachianecti*) are known, a more promising system to investigate in the fossil record is that of the humpback whale lineage and their common barnacle, *Coronula diadema*, as this coronulid species is much more common in the fossil record and is known from more than a dozen sites worldwide (16–21).

Here we investigate the potential of using fossil coronulid $\delta^{18}O$ values to gain insight into the migratory behaviors of prehistoric mysticete whales. Because the majority of the coronulid fossil record belongs to *C. diadema*, an important first step is to establish the reliability with which $\delta^{18}O$ profiles from this species accurately reflect a host whale's migration; we address this by analyzing modern *C. diadema* shells collected from whales with known migration routes. We then analyze Pleistocene-aged

Significance

Migration has long been hypothesized to have played a critical role in baleen whale evolution, but fossil constraints on the history of migration are sparse. Here we provide evidence that the oxygen isotope composition of modern whale barnacle shells reliably records migration pathways. We also analyze fossil whale barnacle shells from three Pleistocene localities and show that they display isotope profiles similar to those of modern specimens. Our results indicate the presence of migration among all three ancient whale populations studied and point to the possibility of reconstructing changes in migratory behaviors from the Pliocene to the present.

Author contributions: L.D.T. designed research; L.D.T., A.O., T.J.B., and S.F. performed research; L.D.T., T.J.B., and S.F. analyzed data; and L.D.T., A.O., T.J.B., and S.F. wrote the paper.

The authors declare no conflict of interest.

This article is a PNAS Direct Submission.

[1]To whom correspondence should be addressed. Email: larry.taylor@berkeley.edu.

This article contains supporting information online at www.pnas.org/lookup/suppl/doi:10.1073/pnas.1808759116/-/DCSupplemental.

Published online March 25, 2019.

coronulids from three unlithified, shallow-sediment sites along the eastern Pacific coast.

Results

Modern coronulid $\delta^{18}O$ profiles show absolute values, ranges, and trajectories that are consistent with expectations given the known migratory pathways of their hosts. UCMP 221031 is a *C. diadema* shell collected from a humpback whale that washed ashore on the California coast and is believed to have belonged to the population which migrates between California and the southern Baja Peninsula. The $\delta^{18}O$ profile recovered from this specimen is consistent with the whale feeding in the waters off the California coast during the previous summer before migrating to the waters surrounding the southern Baja Peninsula (Fig. 1). CAS MAM 21691 is a *C. diadema* collected from a humpback whale that washed ashore near Sitka, Alaska. The $\delta^{18}O$ profile recovered is consistent with the host whale's feeding in the waters near southeast Alaska the previous year before migrating to Hawaii, where the majority of Alaskan humpbacks spend their winters (ref. 2 and Fig. 1). Both of these barnacles are quite large (and therefore presumably old) and appear to record an entire migratory cycle. CAS MAM 21149 is a *C. rhachianecti* shell collected from a gray whale that washed ashore in northern California. Its $\delta^{18}O$ profile is consistent with the whale's having died while heading southward from the Bering Sea (California gray whales migrate from the Bering, Chukchi, and Beaufort Seas to breeding grounds along the Baja Peninsula; *SI Appendix*, Fig. S2).

To test $\delta^{18}O$ variability across plates within individual barnacles we sampled two shell plates of UCMP 221031; both plates show very similar profiles (*SI Appendix*, Fig. S3). To test $\delta^{18}O$ variability across barnacles from a single whale we sampled three small *Coronula* specimens (UCMP 221032, 221033, and 221034) that were collected from a single young whale with an unknown migration route. $\delta^{18}O$ profiles from these specimens do not record a full migratory cycle but exhibit generally consistent trends (*SI Appendix*, Fig. S3).

We examined fossil coronulids from Pleistocene-aged sediments of the San Pedro Formation and Bay Point Formation of California and from sediments previously assigned to the Pliocene-aged Burica Formation of Panama, but which we herein assign a Middle to Late Pleistocene age based on the presence of *Emiliana huxleyi* (refs. 22–25 and *SI Appendix*, Fig. S4). $\delta^{18}O$ profiles from four large *C. diadema* specimens from the Burica Peninsula (UCMP 221022, 221028, 221029, and 221030) exhibit trends and ranges similar to modern specimens but average ~0.96‰ more enriched, as would be expected if these barnacles grew during a glacial (Fig. 2 and *SI Appendix*, Fig. S5 and Table S1). Stationary mollusks collected from the same beds yield notably smaller $\delta^{18}O$ ranges (Fig. 2*D* and *SI Appendix*, Fig. S5). Bay Point fossils (SDSNH 102564, 111656, and 114317, all *Coronula*, and 134747, *Cryptolepas*) and San Pedro fossils (SDSNH 50195, *Coronula*, and 30462, *Cryptolepas*) are all small shell fragments and thus yield truncated $\delta^{18}O$ profiles. Nevertheless, $\delta^{18}O$ ranges and trajectories are comparable to those from modern specimens and are on average enriched by ~1.02‰ (Bay Point fossils) and 1.64‰ (San Pedro fossils) (Fig.

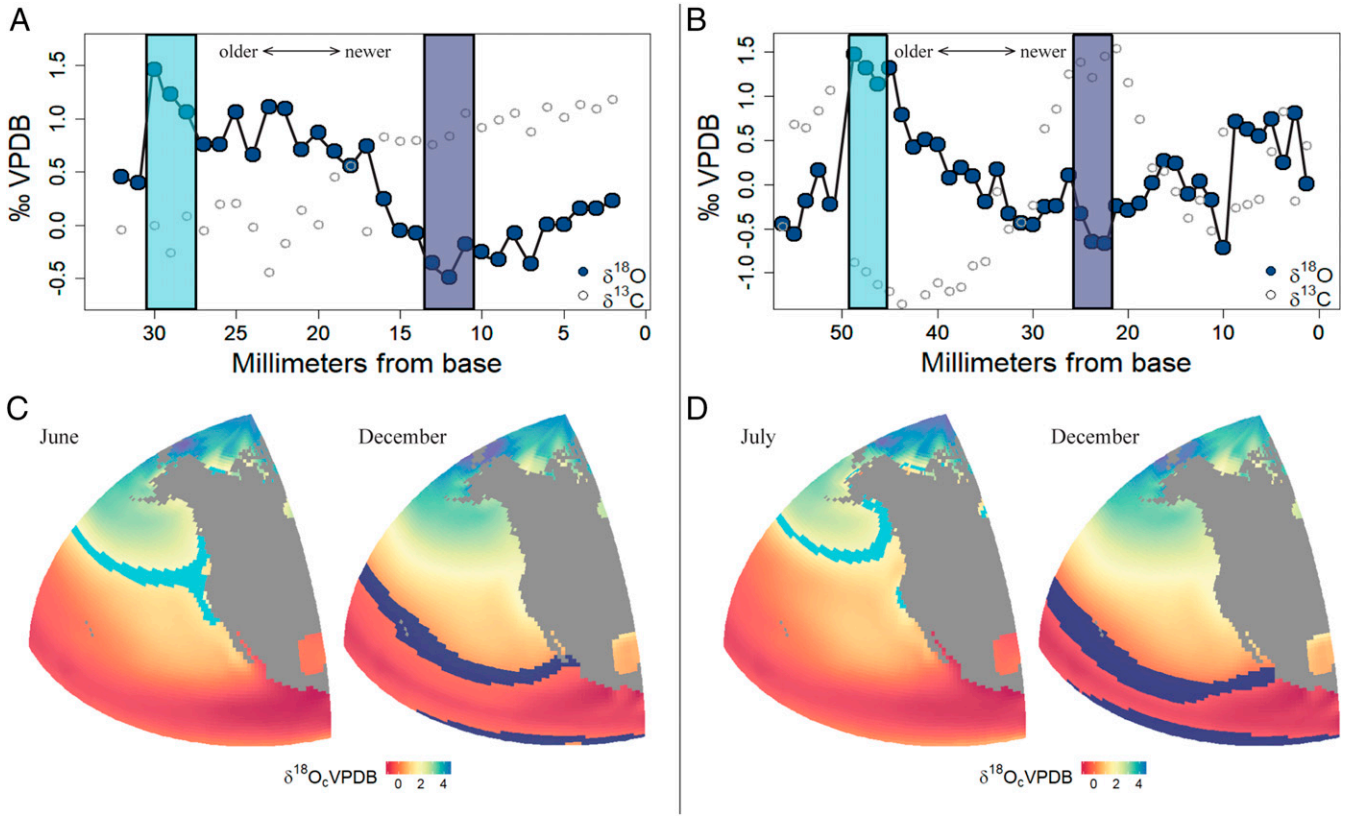

Fig. 1. $\delta^{18}O$ profiles from UCMP 221031 (*A*) and CAS MAM 21691 (*B*), both modern *C. diadema*. UCMP 221031 was collected from a humpback whale that migrated between summer feeding areas along the coast of California and winter breeding areas near the southern Baja Peninsula. Shaded regions of the $\delta^{18}O$ profile (*A*) correspond with shaded regions of plausibility for the whale's location during each season (*C*). CAS MAM 21691 was attached to a humpback whale that migrated between southeast Alaska and Hawaii; shaded regions in *B* align with regions of plausibility in *D*. Analytical precision for this and all other isotopic analyses is ±0.07‰.

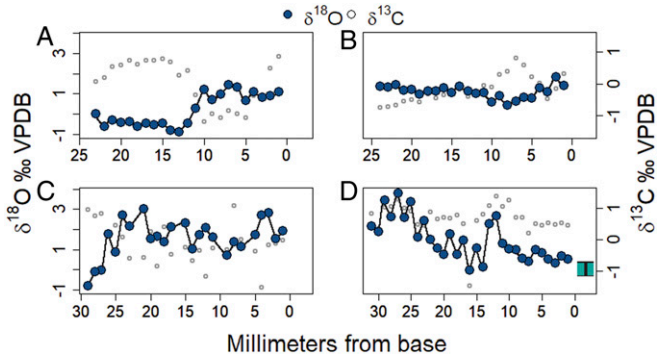

Fig. 2. $\delta^{18}O$ profiles from four Pleistocene-aged *C. diadema* fossils from the Burica Peninsula of Panama. Specimens are UCMP 221029 (*A*), 221030 (*B*), 221022 (*C*), and 221028 (*D*). Blue bar in the right of *D* indicates the range of $\delta^{18}O$ recorded in immobile bivalve shells from the same bedding plane as UCMP 221028. The variety of $\delta^{18}O$ profiles suggests that the whales were migrating to several different feeding regions. This is similar to the modern, where whales that winter off the coast of Panama migrate north to feeding areas from southern California to the Bering Sea and south to the Southern Ocean.

3 and *SI Appendix*, Fig. S5 and Table S1). The exact shape of a $\delta^{18}O$ profile depends on the completeness of the specimen and the direction the host whale was moving in (California fossils, for example, may have come from whales feeding on the California coast, or possibly from those which were only passing by on northward or southward phases of a longer migration).

We examined all specimens for macroscopic indications of possible alteration. Textural and color abnormalities of CASG 78449, a *C. diadema* of poorly constrained age from Mexico, suggest substantial alteration. The $\delta^{18}O$ profile from this specimen is notably depleted relative to all other specimens we analyzed (*SI Appendix*, Fig. S6), which is consistent with open-system alteration in the presence of meteoric waters (26). We used inductively coupled plasma optical emission spectroscopy (ICP-OES) to evaluate trace metal concentrations in four modern coronulids, CASG 78449, and the Burica fossils. Fossil trace metal concentrations are generally not substantially different from the ranges seen in modern coronulids, but some fossils do show modest elevations in iron and manganese (*SI Appendix*, Fig. S7). Scanning electron microscopy of modern coronulids, CASG 78449, and the Burica fossils revealed microscopic indications of alteration in CASG 78449, but not in the other fossils (*SI Appendix*, Fig. S8).

Discussion

J. S. Killingley first recognized the potential of coronulid shell oxygen isotopes to track whale migration, showing that the $\delta^{18}O$ profile of a modern *C. rhachianecti* shell was consistent with expectations based on the migration of its host, a California gray whale (*Eschrichtius robustus*). Here we extend this work by showing that modern $\delta^{18}O$ profiles from the barnacle *C. diadema* reliably reflect the migration paths of host humpback whales (*Megaptera novaeangliae*) and that fossils of both *Cryptolepas* and *Coronula* exhibit $\delta^{18}O$ profiles similar to those of modern individuals.

Interpreting coronulid shell $\delta^{18}O$ begins with understanding their life history. Coronulid growth rates, lifespan, and reproductive strategies are poorly understood due to their unusual habitat. Coronulids are thought to reproduce while their host whales are clustered together for their own breeding (27), and newly settled larvae will eventually grow shells that anchor into mysticete skin so securely that shells may remain attached for some time after the barnacle has died (28). The shells erode at their apex during life (the barnacle retreats downward in response) and thus a shell may not record the barnacle's entire lifespan (28). The largest modern *C. diadema* shells we analyzed record less than 2 y of growth as inferred from progressions between the $\delta^{18}O$ profile's most enriched (corresponding to the whale's feeding season) and most depleted (whale's breeding season) values (Fig. 1); this is in agreement with previous estimates that coronulids live between 1 and 3 y (27, 29).

The largest fossils we analyzed are those from the Burica Peninsula, all of which are relatively complete shells or shell plates. Like modern coronulids, these fossils yield $\delta^{18}O$ profiles with clear signatures of the summer feeding season and winter breeding season (Fig. 2). $\delta^{18}O$ ranges recovered from these fossils equal or exceed those of modern specimens and substantially exceed $\delta^{18}O$ ranges observed in stationary mollusks collected from the same beds (Fig. 2 and *SI Appendix*, Fig. S5). This suggests that the migrations of prehistoric whales was similar in extent to those of today, although a current lack of data on Pleistocene seawater isotopic composition prohibits us from specifying the exact migration paths of these whales. It is notable, however, that the range of $\delta^{18}O$ values seen in these fossils is quite variable (from 1.37‰ to 3.79‰). One possible explanation for this is that Pleistocene whales visiting the Burica Peninsula utilized a variety of different migratory routes. In the present day, whales that winter off the coast of Panama migrate north to feeding grounds which spread from southern California all the way to the northernmost Gulf of Alaska (1, 2). During the southern hemisphere winter, some whales which feed off the coast of Antarctica also migrate to Panama (30, 31). Our results therefore support the interpretation that Panamanian waters have served as a meeting point for whales from a variety of subpopulations for at least the last 270,000 y.

The Bay Point and San Pedro fossils are small shell fragments, with only one of these specimens appearing to capture a full migratory cycle (Fig. 3). The majority instead display a one-way trend in $\delta^{18}O$ values that is interpreted as capturing a portion of the host whale's migration. Even these one-way $\delta^{18}O$ profiles display $\delta^{18}O$ ranges that are too large to be accounted for by annual changes within the region and are therefore taken as reflecting migratory movements of the host whales. While the incompleteness of these profiles makes them more difficult to interpret, they nonetheless display a variety of $\delta^{18}O$ ranges and values. Whales off the California coast include individuals that spend the entire summer feeding in the regional upwelling zones as well as those which pass through on their way to the Pacific Northwest, Alaska, or (in the case of gray whales) even the Bering and Chukchi Seas. The specimen that seems to record a relatively complete migration, a *C. diadema* shell fragment

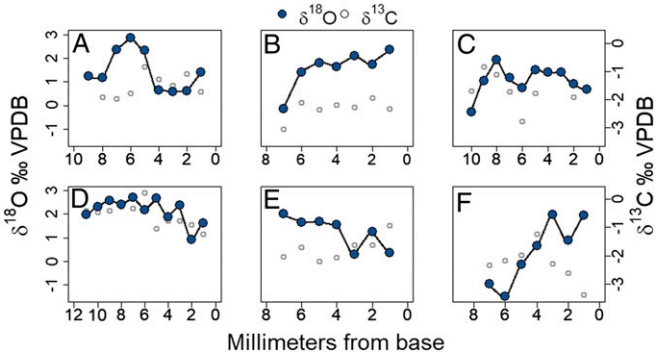

Fig. 3. $\delta^{18}O$ profiles from six Pleistocene-aged coronulid fossils from California. Four are *Coronula* (*A*–*D*) and two are *Cryptolepas* (*E* and *F*). Specimens come from the Bay Point Formation (*A*–*C* and *F*) and San Pedro Formation (*D* and *E*). Specimens are SDSNH 102564 (*A*), 111656 (*B*), 114317 (*C*), 50195 (*D*), 30462 (*E*), and 134747 (*F*).

(SDSNH 102564), yields a $\delta^{18}O$ range of 2.26‰, similar to the modern California *C. diadema* shell (UCMP 221031) which yielded a $\delta^{18}O$ range of 1.95‰ (*SI Appendix*, Table S1). Taken together, our analysis of the Burica and California fossils confirms the presence of migratory behavior in multiple eastern Pacific mysticete populations belonging to both the humpback and gray whale lineages from three different Pleistocene time points.

Both the modern and fossil coronulids yield $\delta^{18}O$ profiles with a continuous progression between the most enriched and depleted values (noting that smaller fossils do not appear to record the full migratory cycle). These progressions sometimes display excursions from the primary $\delta^{18}O$ trend, which may be caused by the whale's passing through waters that locally depart from the route's overall seawater temperature or $\delta^{18}O$ gradients. For example, positive $\delta^{18}O$ excursions against the $\delta^{18}O$ profile's primary trends can occur if the whale passes through either a region of temporarily lower temperature (such as a localized upwelling zone) or a region of high evaporation (preferential evaporation of ^{16}O leaves the water enriched in ^{18}O). Negative $\delta^{18}O$ excursions may occur if the whale's route passed through locally warmer regions or into coastal settings influenced by freshwater runoff, which can create localized depletions of 1 to 3‰ in seawater $\delta^{18}O$ values extending more than a dozen kilometers offshore (32).

Low-Mg calcite is less prone to diagenetic alteration than other biogenic carbonates, and our fossils come from shallow, unlithified sediments, but some fossils nonetheless show modest enrichments in Fe and Mn (*SI Appendix*, Fig. S7), which can be indicators of diagenetic alteration (33, 34). Although this suggests that they may have experienced some diagenetic alteration in the presence of reducing groundwaters, there is little indication that $\delta^{18}O$ profiles are pervasively altered (with the exception of CASG 78449). While recrystallization in the presence of meteoric waters typically causes depletions in bulk $\delta^{18}O$, the Burica, Bay Point, and San Pedro fossils all have $\delta^{18}O$ values which are enriched relative to modern coronulid values, which is an unlikely outcome of independent diagenetic histories. These $\delta^{18}O$ profiles are also coherent and fall within ranges compatible with growth during the glacial Pleistocene, which is hard to reconcile with any major alteration. SEM imaging revealed homogenous, comparable external shell structure between modern coronulids and the Burica fossils (*SI Appendix*, Fig. S8). In contrast, CASG 78449 displays textural and color indications of alteration, has considerable loss or morphing of delicate shell structure, and has a $\delta^{18}O$ profile substantially depleted relative to all other coronulids analyzed (*SI Appendix*, Fig. S6). SEM imaging of CASG 78449 displays evidence of dissolution, pitting, and crystalline overgrowth (*SI Appendix*, Fig. S8).

Several different factors may influence calcite $\delta^{13}C$, including the incorporation of metabolic carbon, kinetic disequilibrium effects, temperature-dependent fractionation, and the $\delta^{13}C$ of dissolved inorganic carbon, which itself can be modified by upwelling or freshwater input. Interpreting $\delta^{13}C$ data is best done alongside accompanying $\delta^{18}O$ values (15, 35–37). Depleted $\delta^{13}C$ values coupled with an enrichment in $\delta^{18}O$ may indicate time spent in an upwelling environment (35, 37), while relatively enriched $\delta^{13}C$ values may correspond to periods spent in more open ocean environments (15). In our coronulid shells, the most enriched $\delta^{18}O$ values often coincide with some of the most depleted $\delta^{13}C$ values, whereas depleted $\delta^{18}O$ values are often paired with relatively enriched $\delta^{13}C$ values; this pattern may signify time that the host whale spent feeding in productive upwelling zones vs. time spent migrating across open ocean environments or in breeding areas with little upwelling. While these broad patterns describing the relationship between $\delta^{18}O$ and $\delta^{13}C$ profiles are true for the majority of the coronulids we analyzed, they are not true for all of them, indicating that the other factors are likely playing a large role in determining coronulid shell $\delta^{13}C$.

It has been suggested that mysticetes first began to migrate in the Plio-Pleistocene (6–8) as productivity became increasingly seasonal (5), clustered within high-latitude waters (38, 39), and repeatedly redistributed by glacial–interglacial cycles (40–42), possibly providing a selective advantage for migration as a means of reliably accessing ephemeral and far-flung resources. Gigantism became established at the same time, allowing for more efficient long-distance travel and enabling mysticetes to better utilize pulses of intense productivity followed by long periods of fasting (6, 43, 44). Our findings demonstrate that migration has been established across multiple whale populations for at least the last several hundred thousand years. Isotopic analysis of other fossil coronulids—which are known from more than a dozen sites across six continents and from sediments dating back to the late Pliocene—provides a promising approach for answering long-standing questions about mysticete behavior and evolution. Combining fossil coronulid $\delta^{18}O$ profiles with paleoceanographic models and emerging proxies that can independently constrain seawater temperature and isotopic composition may provide further constraints on prehistoric migratory pathways.

Materials and Methods

Modern coronulid specimens were previously collected by members of the National Oceanic and Atmospheric Administration's Marine Mammal Stranding Network at the San Diego Natural History Museum (SDNHM) and the California Academy of Sciences (CAS) before being donated to the University of California Museum of Paleontology; several modern specimens were also loaned from the existing collections at the CAS. Some fossil specimens were loaned from the SDNHM and the CAS, and more fossil specimens were collected on the Burica Peninsula of Panama. Modern and fossil specimens from the CAS have specimen labels beginning with "CAS"; SDNHM fossil labels begin with "SDSNH," for the San Diego Society of Natural History.

Depending on the size of the shell, a Dremel hand drill or a New Wave Systems micromill was used to collect calcite samples from along the primary (vertical) growth axis of the shell. Samples of 50 to 100 μg were collected at roughly 1-mm intervals then were analyzed at the Center for Stable Isotope Biogeochemistry at the University of California, Berkeley with a GV IsoPrime mass spectrometer with Dual-Inlet and MultiCarb systems. Several replicates of one international standard NBS19 and two laboratory standards CaCO3-I and II were measured along with every run of samples. Overall external analytical precision is ±0.07‰ for $\delta^{18}O$. Retrieved oxygen isotope profiles are interpreted using the balanomorph-specific paleotemperature equation of Killingley and Newman (13).

To assess if coronulid shells reliably record an isotopic signature of whale movements we compared isotope profiles from modern coronulids against expectations based on their host whales' known migratory route. To do this, we created gridded maps which predict what the average $\delta^{18}O$ of barnacle calcite formed at any point in the ocean should be during each month of the year. Barnacle calcite $\delta^{18}O$ is determined by both the temperature and $\delta^{18}O$ of the seawater in which it forms, as described by Killingley and Newman's equation (13):

$$t(°C) = 22.14 - 4.37(\delta_C - \delta_W) + 0.07(\delta_C - \delta_W)^2,$$

where δ_C denotes barnacle calcite $\delta^{18}O$ and δ_W denotes seawater $\delta^{18}O$. We downloaded global seawater $\delta^{18}O$ (45) and monthly seawater temperature (46) data derived from direct observations coupled with oceanographic models then merged these datasets in R (47). National Oceanic and Atmospheric Administration (NOAA)_Optimum Interpolation (OI)_Sea Surface Temperature (SST) data provided by the NOAA Office of Oceanic and Atmospheric Research, Earth System Research Laboratory, Physical Sciences Division, Boulder, CO (https://www.esrl.noaa.gov/psd/). With the two variables determining barnacle shell $\delta^{18}O$ thus known, we then used the paleotemperature equation to back out predicted barnacle calcite $\delta^{18}O$ for each unit of a map. We created a series of maps indicating the expected $\delta^{18}O$ of barnacle calcite produced in each unit of the map grid; we generated these maps for each month of the year (*SI Appendix*, Fig. S8). We then used these maps to assess whether the $\delta^{18}O$ profiles recovered from modern coronulid shells aligned with expectations based on the host whale's migration route. We used the $\delta^{18}O$ profile's three to four most enriched and most depleted

consecutive values as expectations of where the whale should be during the summer feeding season and winter breeding season, respectively. Because our temperature data are monthly, the number of data points used was chosen so as to represent 1 mo assuming constant growth rates of the barnacle. Because of the latitudinal difference in the whale's feeding and breeding regions, the barnacle experiences the coldest waters in the summer feeding season. Although this will also generally correspond with the lowest seawater $\delta^{18}O$, the temperature-dependent fractionation in barnacles (and other calcifying organisms) generates an enriched shell calcite $\delta^{18}O$ in cold temperatures and a depleted $\delta^{18}O$ in warm temperatures.

Fossils analyzed from California museum collections come from the Pleistocene-aged San Pedro Formation and Bay Point Formation of southern California (23–25), along with one specimen from an unrecorded location in mainland Mexico. Further fossil specimens were collected from shallow marine sediments in the eastern Burica Peninsula of Panama, which were previously believed to belong to the Pliocene-aged Burica Formation (22); bulk samples from this unit were collected for analysis of calcareous nannoplankton assemblages to further constrain ages. Smear slides were prepared using standard techniques and viewed at a magnification of 1250 using a Zeiss Axioskop light microscope. Samples were also observed in a FEI Nova NanoSEM 630 FE scanning electron microscope in the Pennsylvania State University Materials Characterization Laboratory. $\delta^{18}O$ profiles recovered from all fossil coronulids were qualitatively compared against the modern profiles to assess evidence of migration.

All fossil specimens were examined for macroscopic indications (color and texture) of alteration. External shell samples from modern coronulids and the Burica fossils were also imaged with a Hitachi TM-1000 scanning electron microscope for microscopic indications of alteration. We used ICP-OES to compare the trace metal concentrations in the Burica fossils and CASG 78449. The smaller Bay Point and San Pedro fossils, loaned by the San Diego Natural History Museum, were not large enough to be subjected to these analyses without destroying the specimens.

ACKNOWLEDGMENTS. We thank Tom Demere and Kesler Randall (San Diego Natural History Museum), Moe Flannery, Christina Piotrowski, and the late Jean Demouthe (California Academy of Sciences), and Nick Pyenson (Smithsonian National Museum of Natural History) for contributing specimens to this study; Paul Taylor, Ethan Grossman, and Abigail Kelly for their help in the field; Wenbo Yang, Todd Dawson, and Stefania Mambelli (Center for Stable Isotope Biogeochemistry) for their help with all isotope analysis; the staff at the University of California, Berkeley Electron Microscope Laboratory for advice and assistance in electron microscopy sample preparation and data collection; and Valerie and Bill Anders for their generous support. This study was supported by NSF Grant EAR-1325683 and the National System of Investigators (National Secretariat for Science, Technology and Innovation) (to A.O.), by the David and Lucile Packard Foundation (S.F.), and by funding from the Paleontological Society, the Geological Society of America, Sigma Xi, and the University of California Museum of Paleontology (L.D.T.).

1. Calambokidis J, Steiger G, Straley J, Herman L, Cerchio S (2001) Movements and population structure of humpback whales in the North Pacific. *Mar Mamm Sci* 17: 769–794.
2. Calambokidis J, et al. (2009) SPLASH: Structure of populations, levels of abundance and status of humpback whales in the North Pacific. Final report for contract AB133F-03-RP-0078 (Cascadia Research, Olympia, WA).
3. Benson SR, Croll DA, Marinovic BB, Chavez FP, Harvey JT (2002) Changes in the cetacean assemblage of a coastal upwelling ecosystem during El Nino 1997–98 and La Nina 1999. *Prog Oceanogr* 54:279–291.
4. Marlow JR, Lange CB, Wefer G, Rosell-Mele A (2000) Upwelling intensification as part of the Pliocene-Pleistocene climate transition. *Science* 290:2288–2291.
5. Ravelo AC, Andreasen DH, Lyle M, Olivarez Lyle A, Wara MW (2004) Regional climate shifts caused by gradual global cooling in the Pliocene epoch. *Nature* 429:263–267.
6. Slater GJ, Goldbogen JA, Pyenson ND (2017) Independent evolution of baleen whale gigantism linked to Plio-Pleistocene ocean dynamics. *Proc Biol Sci* 284:20170546.
7. Marx FG, Fordyce RE (2015) Baleen boom and bust: A synthesis of mysticete phylogeny, diversity and disparity. *R Soc Open Sci* 2:140434.
8. Berger WH (2007) Cenozoic cooling, Antarctic nutrient pump, and the evolution of whales. *Deep Sea Res Part II Top Stud Oceanogr* 54:2399–2421.
9. McMahon KW, Hamady LL, Thorrold SR (2013) A review of ecogeochemistry approaches to estimating movements of marine animals. *Limnol Oceanogr* 58:697–714.
10. Matthews CJD, Longstaffe FJ, Ferguson SH (2016) Dentine oxygen isotopes (δ (18)O) as a proxy for odontocete distributions and movements. *Ecol Evol* 6:4643–4653.
11. Collareta A, et al. (2018) New insights on ancient cetacean movement patterns from oxygen isotope analyses of a Mediterranean Pleistocene whale barnacle. *Neues Jahrb Geol Palaontol Abh* 288:143–159.
12. Hayashi R, et al. (2013) Phylogenetic position and evolutionary history of the turtle and whale barnacles (Cirripedia: Balanomorpha: Coronuloidea). *Mol Phylogenet Evol* 67:9–14.
13. Killingley JS, Newman WA (1982) 18O fractionation in barnacle calcite: A barnacle paleotemperature equation. *J Mar Res* 40:893–902.
14. Killingley JS (1980) Migrations of California gray whales tracked by oxygen-18 variations in their epizoic barnacles. *Science* 207:759–760.
15. Killingley JS, Lutcavage M (1983) Loggerhead turtle movements reconstructed from 18O and 13C profiles from commensal barnacle shells. *Estuar Coast Shelf Sci* 16: 345–349.
16. Fleming CA (1959) A Pliocene whale barnacle from Hawke's Bay, New Zealand. *N Z J Geol Geophys* 2:242–247.
17. Bianucci G, Di Celma C, Landini W, Buckeridge J (2006) Palaeoecology and taphonomy of an extraordinary whale barnacle accumulation from the Plio-Pleistocene of Ecuador. *Palaeogeogr Palaeoclimatol Palaeoecol* 242:326–342.
18. Buckeridge JS (1983) Fossil barnacles (Cirripedia: Thoracica) of New Zealand and Australia. *N Z Geol Surv Paleontol Bull* 50:1–151.
19. Zullo VA (1969) Thoracic Cirripedia of the San Diego formation, San Diego County, California. *Contrib Sci* 159:1–25.
20. Beu AG (1971) Further fossil whale barnacles from New Zealand. *N Z J Geol Geophys* 14:898–904.
21. Dominici S, Bartalini M, Benvenuti M, Balestra B (2011) Large kings with small crowns: A Mediterranean Pleistocene whale barnacle. *Boll Soc Paleontol Ital* 50:95–101.
22. Moore GW, Kennedy MP (1975) Quaternary faults at San Diego Bay, California. *J Res US Geol Surv* 3:589–595.
23. Wehmiller JF, et al. (1977) Correlation and chronology of Pacific Coast marine terrace deposits of continental United States by fossil amino acid stereochemistry technique evaluation relative ages kinetic model ages and geologic implications. Open-File Report 77-680 (US Geological Survey, Reston, VA).
24. Bryant ME (1987) Emergent marine terraces and quaternary tectonics, Palos Verdes Peninsula, California. *Geology of the Palos Verdes Peninsula and San Pedro Bay: Volume and Guidebook*, eds Fischer PJ, et al. (Society of Economic Paleontologists and Mineralogists, Tulsa, OK), pp 63–78.
25. Coates AGC, et al. (1992) Closure of the Isthmus of Panama: The near-shore marine record of Costa Rica and western Panama. *Geol Soc Am Bull* 104:814–828.
26. Tucker ME, Wright VP (2008) *Carbonate Sedimentology* (Blackwell Scientific, Oxford).
27. Best PB (1991) The presence of coronuline barnacles on a southern right whale Eubalaena australis. *S Afr J Mar Sci* 11:585–587.
28. Seilacher A (2005) Whale barnacles: Exaptational access to a forbidden paradise. *Paleobiology* 31:27–35.
29. Monroe R (1981) Studies in the Coronulidae (Cirripedia): Shell morphology, growth, and function, and their bearing on subfamily classification. *Mem Queensl Mus* 20: 237–251.
30. Acevedo-Gutierrez A, Smultea MA (1995) First records of Humpback whales including calves at Golfo Dulce and Isla del Coco, Costa Rica, suggesting geographical overlap of northern and southern hemisphere populations. *Mar Mamm Sci* 11:554–560.
31. Rasmussen K, et al. (2007) Southern hemisphere humpback whales wintering off Central America: Insights from water temperature into the longest mammalian migration. *Biol Lett* 3:302–305.
32. Khim BK, Krantz DE, Cooper LW, Grebmeier JM (2003) Seasonal discharge of estuarine freshwater to the western Chukchi Sea shelf identified in stable isotope profiles of mollusk shells. *J Geophys Res* 108:3300–3309.
33. Land LS (1967) Diagenesis of skeletal carbonates. *J Sediment Petrol* 37:914–930.
34. Brand U, Veizer J (1980) Chemical diagenesis of a multicomponent carbonate system–1: Trace elements. *J Sediment Petrol* 50:1219–1236.
35. Sadler J, et al. (2012) Reconstructing past upwelling intensity and the seasonal dynamics of primary productivity along the Peruvian coastline from mollusk shell stable isotopes. *Geochem Geophys Geosyst* 13:Q01015.
36. Killingley JS, Berger WH (1979) Stable isotopes in a mollusk shell: Detection of upwelling events. *Science* 205:186–188.
37. Bemis BE, Geary DH (1996) The usefulness of bivalve stable isotope profiles as environmental indicators: Data from the Eastern Pacific Ocean and the Southern Caribbean Sea. *Palaios* 11:328–339.
38. Barron JA, Lyle M, Koizumi I (2002) Late Miocene and early Pliocene biosiliceous sedimentation along the California margin. *Rev Mex Cienc Geol* 19:161–169.
39. Barron JA (1998) Late Neogene changes in diatom sedimentation in the North Pacific. *J Asian Earth Sci* 16:85–95.
40. Martínez-García A, et al. (2014) Iron fertilization of the Subantarctic ocean during the last ice age. *Science* 343:1347–1350.
41. Kumar N, et al. (1995) Increased biological productivity and export production in the glacial Southern Ocean. *Nature* 378:675–680.
42. Lisiecki LE, Raymo ME (2007) Plio–Pleistocene climate evolution: Trends and transitions in glacial cycle dynamics. *Quat Sci Rev* 26:56–69.
43. Goldbogen JA, et al. (2017) How baleen whales feed: The biomechanics of engulfment and filtration. *Annu Rev Mar Sci* 9:367–386.
44. Williams TM (1999) The evolution of cost efficient swimming in marine mammals: Limits to energetic optimization. *Philos Trans R Soc Lond B Biol Sci* 354:193–201.
45. Schmidt GA, Bigg GR, Rohling EJ (1999) Global Seawater Oxygen-18 Database. V1.22. Available at https://data.giss.nasa.gov/o18data/. Accessed March 1, 2016.
46. Reynolds RW, et al. (2002) An improved in situ and satellite SST analysis for climate. *J Climate* 15:1609–1625.
47. R Core Team (2016) R: A language and environment for statistical computing (R Foundation for Statistical Computing, Vienna). Available at https://www.R-project.org/. Accessed March 1, 2016.